

, Accepted 18th May 2018

# Formation of a long-lived radical pair in a Sn(IV) porphyrin–di(L-tyrosinato) conjugate driven by proton-coupled electron-transfer†

Mirco Natali, \*<sup>a</sup> Agnese Amati,<sup>b</sup> Nicola Demitri<sup>c</sup> and Elisabetta Iengo\*<sup>b</sup>

**The novel conjugate 1, featuring two L-tyrosinato residues axially coordinated to the tin centre of a Sn(IV)-tetraphenylporphyrin, is reported as the first example of a supramolecular dyad for photochemical PCET. It is noteworthy that the excitation of 1 in the presence of a suitable base is followed by photoinduced PCET leading to a radical pair state with a surprisingly long lifetime.**

Artificial photosynthesis (AP), that is conversion of solar energy into chemical fuels, represents a viable, yet challenging solution in response to the global energy issue.<sup>1</sup> In a biomimetic approach, any artificial photosynthetic scheme must envision a charge-separating system wherein light-absorption triggers a series of electron transfer (ET) processes eventually leading to a spatial separation of an electron and a hole (radical pair).<sup>2</sup> The achievement of a long-lived charge separation is essential in order to couple the photoinduced one-electron transfer processes with the dark multi-electron catalytic steps, namely conversion of substrates (e.g., H<sub>2</sub>O, CO<sub>2</sub>, etc.) into fuels (e.g., H<sub>2</sub>, CO, CH<sub>3</sub>OH, etc.).<sup>2,3</sup> In the electron transport chain of natural photosystem II (PSII) oxidation of the tyrosine donor (Y<sub>2</sub>) and reduction of the quinone acceptor (Q<sub>B</sub>), after light absorption by chlorophyll P680, are both coupled to the transfer of protons (proton-coupled electron-transfer, PCET) that help in stabilizing the radical pair state from both thermodynamic and kinetic standpoints.<sup>4,5</sup> Hence, in a biomimetic fashion, several artificial systems have been recently investigated based on PCET.<sup>6–8</sup> However, the systems reported so far are all covalent in nature, thus requiring

demanding synthetic protocols and impeding the use of simple and reliable comparative models.

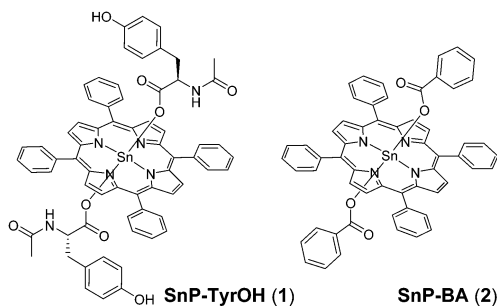
On the other hand, the well-documented selective reactivity of Sn(IV)-di(hydroxo)-porphyrins towards the carboxylic functional group, leading to symmetric Sn(IV)-di(carboxylate)-porphyrin complexes with total conversions,<sup>9</sup> has been pursued by us and others as a metal-mediated strategy to target photoactive dyads (or pseudo-triads).<sup>10</sup> The supramolecular character of these conjugates, common to other metallo-porphyrin metal-mediated derivatives,<sup>11</sup> combined with the distinguished robustness of the Sn(IV)-carboxylate axial bonds and the antenna/redox properties of tin-porphyrins forecast the possibility of accessing valuable photoinduced charge separated states by exploiting combinatorial screening of different chromophore/carboxylate partners.<sup>10</sup> In fact, the combinatorial flexibility offered by these conjugates joined with the large databases on the opto-electronic properties of structural alternative components may allow for viable predictions of the photoinduced reactivity, as well as the design and facile preparation of multiple photochemical systems. However, the kinetic limitations, namely fast charge recombination, have been, so far, difficult to overcome. In this regard, we present here the first pioneering system based on the successful merging of Sn(IV)-porphyrin metal-mediation with proton-coupled electron-transfer by exploiting the well-established PCET reactivity of the phenol group.<sup>12</sup> Quite unexpectedly, **1** is only the third reported example of derivatives in which chiral amino acid residues are connected to a tin-porphyrin chromophore by metal mediation,<sup>13</sup> and their use as synthons in the supramolecular realm, while intriguing, is yet unexplored.

SnP-TyrOH (**1**, Scheme 1) was easily prepared from readily available starting materials by a method recently reported by us and adapted from literature procedures.<sup>9,10</sup> A 1:2 mixture of *trans*-dihydroxo(5,10,15,20-tetraphenylporphyrinato)-tin(IV) and *N*-acetyl-L-tyrosine was kept under refluxing conditions, in CHCl<sub>3</sub>, for 12 hours. Solvent evaporation followed by recrystallization of the crude with a CHCl<sub>3</sub>/acetone/*n*-hexane mixture afforded the desired product as a pure microcrystalline material, in quantitative yield. **1** was unambiguously characterized with a

<sup>a</sup> Department of Chemical and Pharmaceutical Sciences, University of Ferrara and Centro Interuniversitario per la Conversione Chimica dell'Energia Solare (SOLARCHEM), Via L. Borsari 46, 44121 Ferrara, Italy. E-mail: mirco.natali@unife.it

<sup>b</sup> Department of Chemical and Pharmaceutical Sciences, University of Trieste, Via L. Giorgieri 1, 34127 Trieste, Italy. E-mail: eiengo@units.it

<sup>c</sup> Elettra-Sincrotrone Trieste, S.S. 14 Km 163.5 in Area Science Park, 34149 Basovizza, Trieste, Italy



Scheme 1 Molecular structures of conjugate **1** and model compound **2**.

variety of techniques, with all the data confirming the presence of two amino acid residues axially bound to the metal centre of one tin-porphyrin *via* the carboxylate groups (see the ESI† for full details). A distinguishing feature of **1** is that of being chiral, as nicely evidenced by the induced CD signal observed in the absorption region (Soret-band) of the metallo-porphyrin (Fig. S5, ESI†). This fingerprint is observed under diluted conditions (25  $\mu\text{M}$  of **1** in  $\text{CH}_2\text{Cl}_2$ ), thus confirming the stability in the solution of **1**, as already documented for related tin-porphyrin adducts,<sup>9,10</sup> and ensuring the integrity of the conjugate in the photophysical studies (see below). Single crystals were obtained by slow diffusion of *n*-hexane into a  $\text{CHCl}_3$ /acetone solution of **1**, the resulting X-ray structure (Fig. 1 and Fig. S6–S8, ESI†) confirms the expected  $C_2$  stereocenter (S) configurations and evidences ordered patterns of intermolecular H-bonds.

Comparison of the optical and cyclic voltammetry data in  $\text{CH}_2\text{Cl}_2$  for **1**, SnP-BA (**2**) (Scheme 1), and *N*-acetyl-L-tyrosine (see absorption and emission spectra in Fig. S9–S11, ESI† and Table 1) evidences the absence of relevant ground state electronic interactions between the amino acid and the tin-porphyrin components in **1**. This supramolecular feature, well documented in previous reports by us and others,<sup>10,11</sup> legitimates the use of **2** and the free amino acid as reliable comparative models. In particular, from these data it is possible to confidently anticipate that, on simple thermodynamic grounds, both singlet and triplet excited states of the tin-porphyrin are not sufficiently high in energy to promote oxidation of the attached tyrosine in pure  $\text{CH}_2\text{Cl}_2$  (see the ESI†). Indeed, comparable emission profiles, in terms of spectral shape and intensities (Fig. S11, ESI†), are found upon excitation of optically matched solutions of **1** and **2**. Also, similar fluorescence lifetimes ( $\tau \approx 1.15$  ns, Fig. S12, ESI†) are measured in both cases. Similarly, the triplet excited state of

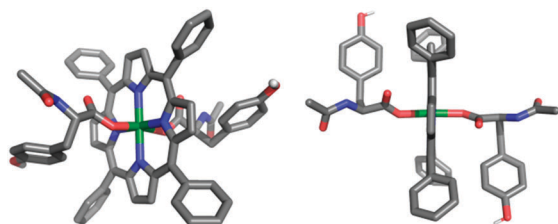


Fig. 1 Two views of the single crystal X-ray structure of **1**, solvent molecules and hydrogens, except for those of the OH groups, are omitted for clarity. Color code: H, white; C, gray; N, blue; O, red; Sn, green.

Table 1 Electrochemical data<sup>a</sup>

	$E_{\text{ox}}$ (V)	$E_{\text{red}}$ (V)
<b>1</b>	+0.89 <sup>b,c</sup>	-1.40
<b>2</b>	+0.91	-1.37
<i>N</i> -Acetyl-L-tyrosine	+0.83 <sup>b</sup>	—

<sup>a</sup> Obtained by cyclic voltammetry (CV) in  $\text{N}_2$ -purged  $\text{CH}_2\text{Cl}_2$  (0.1 M TBAPF<sub>6</sub>) at 298 K, scan rate  $\nu = 100$  mV s<sup>-1</sup>, using GC as a WE, Pt as a CE, and SCE as a reference, potentials are referred to Fc/Fc<sup>+</sup> used as an internal standard (Fig. S14 and S15, ESI). <sup>b</sup> Irreversible wave, peak potential given. <sup>c</sup> Process attributed to tyrosine for intensity reasons, SnP oxidation is likely buried under this intense wave.

the Sn(IV) porphyrin in **1**, as detected by flash photolysis (Fig. S13, ESI†), is also comparable in both absorbance and lifetime ( $\tau \approx 2.2$  and  $\tau \approx 35$   $\mu\text{s}$  under air-equilibrated and oxygen-free conditions, respectively) with that of **2**. All these observations confirm negligible quenching of both singlet and triplet excited states of the chromophore and therefore the impossibility for **1** to exhibit inter-component photoinduced processes in pure  $\text{CH}_2\text{Cl}_2$ .

The photophysics of **1** changes dramatically in the presence of an organic base. Addition of pyrrolidine in the range of 0–0.084 M brings about a severe quenching of the SnP fluorescence (Fig. 2) with an efficiency that is dependent on the pyrrolidine concentration and almost saturates above *ca.* 0.05 M base reaching a value of *ca.* 60% (Table S4, ESI†). The fluorescence lifetime decreases along with the emission intensity (Fig. 2b). The observed behaviour can be attributed to the occurrence of a photoinduced PCET from the singlet excited state of the chromophore involving reduction of the porphyrin and oxidation of the tyrosine with a concomitant proton shift from the phenol of the amino acid to the base, according to eqn (1), and presumably taking place *via* a concerted mechanism (CPET).



This process is indeed expected to be exergonic by *ca.* 1.1 eV, as estimated from the electrochemical data in Table 1, the energy of the <sup>1</sup>SnP excited state, and the energy stabilization arising from the deprotonation of the oxidized tyrosine by the base (see the ESI† for details). Most importantly, the hypothesis of a CPET quenching mechanism is strongly supported by the following considerations.‡ (i) Addition of pyrrolidine to a solution of **2** in  $\text{CH}_2\text{Cl}_2$  has almost negligible effects on the SnP fluorescence intensity and lifetime (Fig. S16, ESI†), thus ruling out any alternative ET quenching by the base. (ii) Pyrrolidine

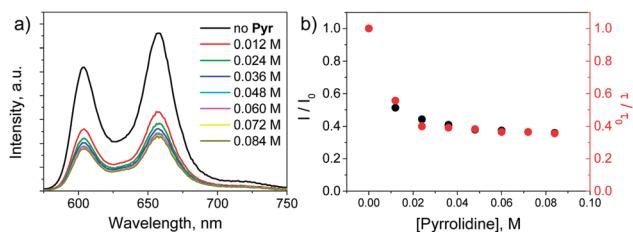


Fig. 2 (a) Emission spectra ( $\lambda_{\text{exc}} = 532$  nm) in  $\text{CH}_2\text{Cl}_2$  solutions containing 25  $\mu\text{M}$  **1** and 0–0.084 M pyrrolidine; (b) trend of  $I/I_0$  and  $\tau/\tau_0$  ratios vs. pyrrolidine concentration.

does not deprotonate the tyrosine hydroxyl moiety as confirmed by absorption measurements (Fig. S17, ESI<sup>†</sup>), thus excluding a simple ET pathway to a putative phenolate. Conversely, the latter observations clearly support the presence of a pre-association equilibrium between the amino acid and the base *via* hydrogen bonding, a fundamental requirement for the occurrence of PCET.<sup>5,7,14</sup> (iii) The kinetic treatment of the quenching data of Fig. 2b, by considering the above-mentioned SnP-TyrOH<sup>•-</sup>·Pyr interaction,<sup>6,15</sup> results in an accurate fitting for a chosen value of association constant of  $K_A = 45(\pm 5) \text{ M}^{-1}$ , in line with the literature data,<sup>15</sup> and a rate constant of  $k_{\text{CPET}} = 2.1(\pm 0.03) \times 10^9 \text{ s}^{-1}$  (see the ESI<sup>†</sup> for detailed analysis). Importantly, the  $K_A$  value so obtained is fully compatible with the value of  $K_A = 47(\pm 7) \text{ M}^{-1}$  independently determined for the hydrogen-bonding association between tyrosine and pyrrolidine in  $\text{CH}_2\text{Cl}_2$  (Fig. S23, ESI<sup>†</sup>).<sup>16</sup> (iv) The prompt transient spectrum detected by laser flash photolysis of **1** with 0.06 M base (Fig. S18, ESI<sup>†</sup>) can be reasonably represented by a combination of differential spectra of the triplet excited state and a fraction of the radical pair state (see the ESI<sup>†</sup>). Indeed, the presence of a more pronounced shoulder at *ca.* 450 nm with respect to the transient spectrum of the triplet only, as measured in **2**, can be possibly attributed to the presence of some SnP radical anion (*i.e.*, one product expected after the process in eqn 1 has occurred, Fig. S18 and S19, ESI<sup>†</sup>).

The fraction of triplet state formed *via* intersystem crossing from the singlet, in competition with the PCET, displays pyrrolidine-dependent deactivation profiles. Progressive additions of the base cause indeed faster decays, as monitored at the transient absorption maximum (Fig. 3a). This evidence is consistent with the occurrence of a quenching process also at the triplet level. Similarly to what was observed for the singlet excited state (Fig. 2b), the pyrrolidine concentration has a remarkable effect on the quenching efficiency (Fig. 3b). Accordingly, this process can be attributed to a parallel CPET originating from the triplet excited state level (eqn (2)).



On the basis of thermodynamic considerations, this process is indeed expected to be exergonic by *ca.* 0.7 eV and can be substantiated by the following arguments.<sup>‡</sup> (i) Bimolecular quenching of the triplet excited state by pyrrolidine, as observed using model **2** (Fig. S20, ESI<sup>†</sup>), is considerably less efficient than

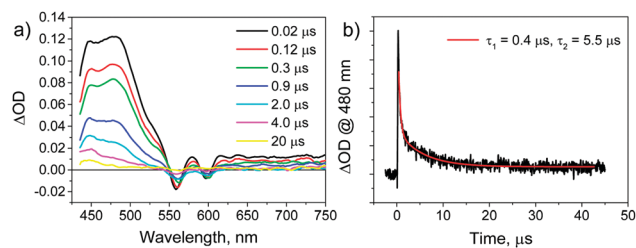


Fig. 4 (a) Spectral evolution of the transient absorption and (b) kinetic trace at 480 nm with related biexponential fitting obtained by laser flash photolysis ( $\lambda_{\text{exc}} = 532 \text{ nm}$ ) in oxygen-free  $\text{CH}_2\text{Cl}_2$  with 25  $\mu\text{M}$  **1** and 0.06 M pyrrolidine.

the quenching process measured in **1**, thus ruling out a direct ET from the pyrrolidine. (ii) Fitting of the kinetic data in Fig. 3b, using the same procedure<sup>6,15</sup> employed for the singlet excited state (see the ESI<sup>†</sup>), is found satisfactory with the same association constant ( $K_A = 45(\pm 5) \text{ M}^{-1}$ ) and a rate of  $k_{\text{CPET}} = 3.4(\pm 0.08) \times 10^6 \text{ s}^{-1}$ .<sup>§</sup> (iii) The spectral evolution of the transient absorption of **1** in the presence of 0.06 M pyrrolidine, as measured by laser flash photolysis under oxygen-free conditions, displays a biphasic behaviour (Fig. 4). In the first process, *ca.* 1  $\mu\text{s}$  ( $\tau_1 = 0.4 \mu\text{s}$ , Fig. 4b), the prompt transient signal, mainly attributable to the triplet excited state (maximum at 480 nm), progressively decays and changes in shape yielding a new transient signal featuring a maximum at 450 nm, attributable to the presence of the SnP radical anion only (Fig. S18b, ESI<sup>†</sup>). In the second process ( $\tau_2 = 5.5 \mu\text{s}$ , Fig. 4b), the latter spectrum decays to the baseline. The first spectral evolution can be safely attributed to the formation of the SnP<sup>-</sup>-TyrO<sup>•-</sup>·<sup>+</sup>HPyr state (the tyrosyl radical is spectroscopically silent in this wavelength range),<sup>7</sup> while the second process corresponds to the ground-state repopulation from the above-mentioned radical pair state (see below). A quantum yield of  $\Phi = \sim 0.3$  can be estimated for the formation of such a PCET photoproduct which definitely points towards a sole triplet contribution (see the ESI<sup>†</sup>). Most importantly, the SnP<sup>-</sup>-TyrO<sup>•-</sup>·<sup>+</sup>HPyr state is considerably long-lived, with a lifetime reaching the  $\mu\text{s}$  time-scale (*ca.* 6  $\mu\text{s}$ ). Notably, this result is rather impressive when compared to both dyad systems displaying photoinduced ET processes, wherein only few exceptions can be found,<sup>18,19</sup> and related two-component systems involving light-driven PCET.<sup>6,7</sup> Interestingly, a comparable, albeit shorter, lifetime has been achieved only in a more complex (covalent) triad system featuring related molecular components.<sup>8</sup>

In summary, upon visible-light excitation of **1** in the presence of pyrrolidine, two radical pair states of the type SnP<sup>-</sup>-TyrO<sup>•-</sup>·<sup>+</sup>HPyr can be populated that differ in terms of spin multiplicity: the first one is formed in the sub-ns regime by singlet quenching and undergoes an extremely fast decay ( $k > 10^8 \text{ s}^{-1}$ ), and the second one has triplet spin multiplicity and is long-lived, as experimentally detected by transient absorption in both its formation and deactivation (Fig. 4).

The overall set of photochemical processes occurring in **1** in  $\text{CH}_2\text{Cl}_2$  in the presence of pyrrolidine is summarized in Fig. 5. Two alternative mechanisms may be available for the ground-state decay from both radical pair states (singlet and triplet):

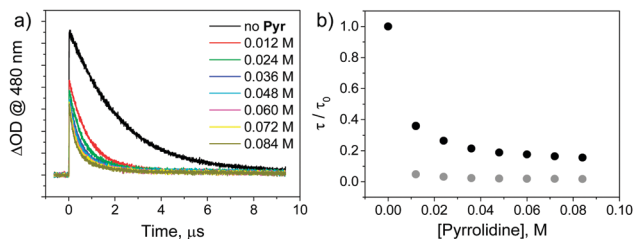


Fig. 3 (a) Kinetic traces at 480 nm obtained by laser flash photolysis ( $\lambda_{\text{exc}} = 532 \text{ nm}$ ) in air-equilibrated  $\text{CH}_2\text{Cl}_2$  solutions containing 25  $\mu\text{M}$  **1** and 0–0.084 M pyrrolidine; (b) trend of  $\tau/\tau_0$  ratio vs. pyrrolidine concentration under air-equilibrated (black dots) and oxygen-free conditions (grey dots).

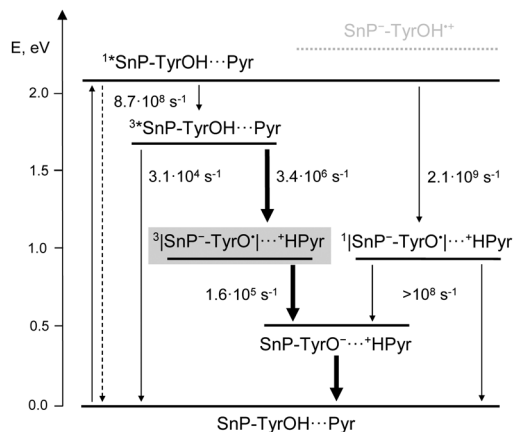
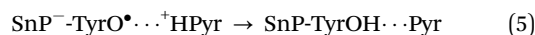
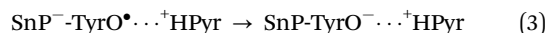


Fig. 5 Energy level diagram in **1** with related photoinduced processes and rates in  $\text{CH}_2\text{Cl}_2$  in the presence of pyrrolidine (see the ESI† for details on the energy levels; for simplicity the same energy is assigned to both singlet and triplet charge transfer states); formation and decay of the long-lived charge separated state are highlighted for guiding the reader.

(i) stepwise ET-PT (eqn (3) and (4)) or (ii) concerted PCET (CPET, eqn (5)).



As for the long-lived triplet radical pair state,<sup>¶</sup> the spectral changes do not allow to unambiguously establish the actual mechanism (the phenolate anion potentially formed *via* eqn (3) has indeed no fingerprint in the visible region, Fig. S17, ESI†). However, the observation of appreciably pyrrolidine-independent kinetics (Table S4 and Fig. S24, ESI†) favours the stepwise ET-PT (eqn (3) and (4)) over the CPET pathway (eqn (5)). Interestingly, this behaviour is similar to that observed in related polypyridine Re(i)/Ru(ii)-phenol dyads<sup>6</sup> where efficient charge separation *via* CPET was actually followed by intramolecular reverse electron transfer. It is noteworthy that, with respect to those systems,<sup>6</sup> the reverse backward ET process (eqn (3)) is herein considerably slower. This evidence can be confidently attributed to the absence of relevant spin-orbit coupling in conjugate **1**, with respect to the ruthenium/rhenium cases,<sup>6</sup> which makes the spin-forbidden, backward reaction substantially slower.<sup>20</sup>

In conclusion, we have reported on the first example of a supramolecular dyad, based on a tin-porphyrin antenna/electron-acceptor and a tyrosine amino acid electron-/proton-donor, that displays a surprisingly long-lived radical pair state when excited in the presence of pyrrolidine. Its formation follows a CPET mechanism mediated by H-bonding between the tyrosyl residues and the base. The present work thus elects the combination of the simple metal-mediated conjugates with the PCET reactivity as an effective turning point within artificial photosynthetic schemes. Also, the symmetric, disubstituted characteristic of Sn(IV) porphyrins (pseudo-triad structural motif) may also potentially lead to light-induced accumulation of multiple redox equivalents *via* PCET.<sup>21</sup> Hence, this novel

interpretation of the supramolecular combinatorial flexibility<sup>11</sup> will offer a unique opportunity for the development of an extended library of new photochemical systems aimed at a better understanding of the fundamental rules governing PCET. Research towards this direction is currently being planned in our labs.

Financial support from the University of Ferrara (FAR 2017) and the University of Trieste (FRA 2016) is gratefully acknowledged.

## Conflicts of interest

There are no conflicts to declare.

## Notes and references

‡ Determination of the H/D kinetic isotope effect may be useful to additionally confirm the CPET mechanism. However, the difficulties in the preparation of the deuterated analogue of **1** by standard literature methods<sup>6</sup> due to the oxophilicity of **1** hampered this type of study at this stage. This issue will be addressed in the near future.

§ The almost 1000-fold difference in rates between singlet and triplet PCET can be mainly imparted to the different  $\Delta G^\circ$  values. Such a difference in rates would be indeed compatible, in a classical Marcus-type treatment assuming comparable pre-exponential factors, with a total reorganization energy of  $\lambda \approx 1.2$  eV (see the ESI†). This value is much larger than that measured, *e.g.*, in a SnP-carboxylate adduct displaying ET only<sup>17</sup> and may further support the PCET nature of both singlet and triplet quenching processes.<sup>5</sup>

¶ The very short lifetime of the singlet radical pair state (see the ESI†) makes a detailed mechanistic analysis not much relevant at this stage and will be discussed elsewhere.

- 1 N. Armaroli and V. Balzani, *Angew. Chem., Int. Ed.*, 2007, **46**, 52.
- 2 B. D. Sherman, M. D. Vaughn, J. J. Bergkamp, D. Gust, A. L. Moore and T. A. Moore, *Photosynth. Res.*, 2014, **120**, 59.
- 3 L. Hammarström, *Acc. Chem. Res.*, 2015, **48**, 840.
- 4 J. L. Dempsey, J. R. Winkler and H. B. Gray, *Chem. Rev.*, 2010, **10**, 7024.
- 5 (a) D. R. Weinberg, C. J. Gagliardi, J. F. Hull, C. F. Murphy, C. A. Kent, B. C. Westlake, A. Paul, D. H. Ess, D. G. McCafferty and T. J. Meyer, *Chem. Rev.*, 2012, **112**, 4016; (b) J. C. Lennox, D. A. Kurz, T. Huang and J. L. Dempsey, *ACS Energy Lett.*, 2017, **2**, 1246.
- 6 (a) M. Kuss-Petermann, H. Wolf, D. Stalke and O. S. Wenger, *J. Am. Chem. Soc.*, 2012, **134**, 12844; (b) M. Kuss-Petermann and O. S. Wenger, *J. Phys. Chem. A*, 2013, **117**, 5726; (c) J. Chen, M. Kuss-Petermann and O. S. Wenger, *Chem. - Eur. J.*, 2014, **20**, 4098; (d) A. Pannwitz and O. S. Wenger, *J. Am. Chem. Soc.*, 2017, **139**, 13308.
- 7 (a) T. Irebo, S. Y. Reece, M. Sjödin, D. G. Nocera and L. Hammarström, *J. Am. Chem. Soc.*, 2007, **129**, 15462; (b) T. Irebo, M.-T. Zhang, T. F. Markle, A. M. Scott and L. Hammarström, *J. Am. Chem. Soc.*, 2012, **134**, 16247; (c) A. A. Pizano, J. L. Yang and D. G. Nocera, *Chem. Sci.*, 2012, **3**, 2457.
- 8 (a) G. F. Moore, M. Hambourger, M. Gervaldo, O. G. Poluektov, T. Rajh, D. Gust, T. A. Moore and A. L. Moore, *J. Am. Chem. Soc.*, 2008, **130**, 10466; (b) J. D. Megiatto, A. Antoniuk-Pablant, B. D. Sherman, G. Kodis, M. Gervaldo, T. A. Moore, A. L. Moore and D. Gust, *Proc. Natl. Acad. Sci. U. S. A.*, 2012, **109**, 15578; (c) S. J. Mora, E. Odella, G. F. Moore, D. Gust, T. A. Moore and A. L. Moore, *Acc. Chem. Res.*, 2018, **51**, 445.
- 9 (a) J. C. Hawley, N. Bampos and J. K. M. Sanders, *Chem. - Eur. J.*, 2003, **9**, 5211; (b) D. P. Arnold and A. Blok, *Coord. Chem. Rev.*, 2004, **248**, 299; (c) V. S. Shetti, Y. Pareek and M. Ravikanth, *Coord. Chem. Rev.*, 2012, **256**, 2816.
- 10 (a) T. Honda, T. Nakanishi, K. Ohkubo, T. Kojima and S. Fukuzumi, *J. Phys. Chem. C*, 2010, **114**, 14290; (b) T. Lazarides, S. Kuhri, G. Charalambidis, M. K. Panda, D. M. Guldi and A. G. Coutsolelos, *Inorg. Chem.*, 2012, **51**, 4193; (c) P. Cavigli, G. Balducci, E. Zangrando, N. Demitri, A. Amati, M. T. Indelli and E. Iengo, *Inorg. Chim. Acta*, 2016, **439**, 61.

- 11 (a) F. Scandola, C. Chiorboli, A. Prodi, E. Iengo and E. Alessio, *Coord. Chem. Rev.*, 2006, **250**, 1471; (b) E. Iengo, G. D. Pantoş, J. K. M. Sanders, M. Orlandi, C. Chiorboli, S. Fracasso and F. Scandola, *Chem. Sci.*, 2011, **2**, 676; (c) M. Natali, R. Argazzi, C. Chiorboli, E. Iengo and F. Scandola, *Chem. – Eur. J.*, 2013, **19**, 9261; (d) A. Amati, P. Cavigli, A. Kahnt, M. T. Indelli and E. Iengo, *J. Phys. Chem. A*, 2017, **121**, 4242.
- 12 (a) J. J. Warren, T. A. Tronic and J. M. Mayer, *Chem. Rev.*, 2010, **110**, 6961; (b) C. Constantin, M. Robert and J.-M. Savéant, *Acc. Chem. Res.*, 2010, **43**, 1019.
- 13 (a) S. H. Kim, H. Kim, K. K. Kim and H. J. Kim, *J. Porphyrins Phthalocyanines*, 2009, **13**, 806; (b) K. Karikis, E. Georgilis, G. Charalambidis, A. Petrou, O. Vakuliuk, T. Chatziioannou, I. Raptaki, S. Tsovola, I. Papakyriacou, A. Mitraki, D. T. Gryko and A. G. Coutsolelos, *Chem. – Eur. J.*, 2016, **22**, 11245.
- 14 S. Hammes-Schiffer and A. A. Stuchebrukhov, *Chem. Rev.*, 2010, **110**, 6939.
- 15 L. Biczòk, N. Gupta and H. Linschitz, *J. Am. Chem. Soc.*, 1997, **119**, 12601.
- 16 P. Dongare, A. G. Bonn, S. Maji and L. Hammarström, *J. Phys. Chem. C*, 2017, **121**, 12569.
- 17 T. Kojima, K. Hanabusa, K. Okhubo, M. Shiro and S. Fukuzumi, *Chem. – Eur. J.*, 2010, **16**, 3646.
- 18 S. Fukuzumi, K. Okhubo and T. Suenobu, *Acc. Chem. Res.*, 2014, **47**, 1455.
- 19 (a) D. Gust, T. A. Moore and A. L. Moore, *Acc. Chem. Res.*, 2001, **34**, 40; (b) F. Wessendorf, B. Grimm, D. M. Guldi and A. Hirsch, *J. Am. Chem. Soc.*, 2010, **132**, 10786; (c) M. Natali, S. Campagna and F. Scandola, *Chem. Soc. Rev.*, 2014, **43**, 4005.
- 20 J. W. Verhoeven, *J. Photochem. Photobiol., C*, 2006, **7**, 40.
- 21 M. Kuss-Petermann, M. Oraziotti, M. Neuburger, P. Hamm and O. S. Wenger, *J. Am. Chem. Soc.*, 2017, **139**, 5225.